

# Circuit-Depth Reduction of Unitary-Coupled-Cluster Ansatz by Energy Sorting

Yi Fan,<sup>1,2</sup> Changsu Cao,<sup>3</sup> Xusheng Xu,<sup>1</sup> Zhenyu Li,<sup>2</sup> Dingshun Lv,<sup>1,\*</sup> and Man-Hong Yung<sup>1,†</sup>

<sup>1</sup>*Central Research Institute, 2012 Labs, Huawei Technologies*

<sup>2</sup>*Hefei National Laboratory for Physical Sciences at the Microscale,*

*University of Science and Technology of China, Hefei, Anhui 230026, China*

<sup>3</sup>*Tsinghua University, Department of Chemistry, Beijing 100084, China*

(Dated: June 30, 2021)

Quantum computation represents a revolutionary means for solving problems in quantum chemistry. However, due to the limited coherence time and relatively low gate fidelity in the current noisy intermediate-scale quantum (NISQ) devices, realization of quantum algorithms for large chemical systems remains a major challenge. In this work, we demonstrate how the circuit depth of the unitary coupled cluster ansatz in the algorithm of variational quantum eigensolver can be significantly reduced by an energy-sorting strategy. Specifically, subsets of excitation operators are pre-screened from the unitary coupled-cluster singles and doubles (UCCSD) operator pool according to its contribution to the total energy. The procedure is then iteratively repeated until the convergence of the final energy to within the chemical accuracy. For demonstration, this method has been successfully applied to systems of molecules and periodic hydrogen chain. Particularly, a reduction up to 14 times in the number of operators is observed while retaining the accuracy of the origin UCCSD operator pools. This method can be widely extended to other variational ansatz other than UCC.

## I. INTRODUCTION

Noisy intermediate-scale quantum(NISQ) devices [1] have been studied extensively to demonstrate a variety of small-scale quantum computations. In particular, the ground-state problem of quantum chemistry is one of the applications that can potentially achieve exponential speed-up on quantum computers [2, 3]. Quantum phase estimation (QPE) and variational quantum eigensolver (VQE) are two dominant algorithms to solve for the ground-state of a chemical system. QPE implements the time evolution operator  $U = e^{i\hat{H}t}$  and evolves the Hamiltonian of the molecule in time on a quantum computer [4] to obtain the energy spectrum with accuracy comparable to full configuration interaction (FCI)[5–11]. However, accurate QPE simulation requires long coherence time, high (two-qubit) gate fidelity and even error correction devices, which is far beyond the NISQ era. In contrast to QPE, VQE[12, 13] embeds efficient quantum simulations into a classical optimization process, which yields a much shallower circuit and thus relieves the requirement of coherence time and gate fidelity. In the procedure of VQE, a trial wave function is constructed on the quantum computer, depending on a set of classical parameters and the energy is estimated by measuring the expectation values of the Hamiltonian. On the classical computer, the parameters are optimized and updated to minimize the energy. VQE was first experimentally demonstrated on a photonic quantum processor[13] to study the ground state of  $\text{HeH}^+$ . Lots of experiments have been carried out on leading platforms, including superconductor quantum processor[11, 14–16] and trapped-ion quantum processor[17–19].

The main ingredient of VQE is the appropriate choice of the wave function ansatz. Most commonly used schemes include physically motivated ansatz (PMA) based on systematic techniques to approximate the exact wave function, such as the unitary coupled-cluster theory[11, 17–21], and hardware heuristic ansatz (HHA) which considers specific hardware structure and employs entangling blocks, such as the hardware efficient ansatz[14]. Although VQE greatly lowered the requirement of quantum resource and showed promising applications in quantum chemistry simulations, the robustness is achieved at the expense of increased number of measurements. One of the main concerns of VQE is to find a shallower parametric quantum circuit to generate a compact wave function ansatz meanwhile retaining an acceptable accuracy. The parameter space should be small enough to enable fast convergence [22]. Recent studies have been carried out with the goal of obtaining a compact and parameter-efficient ansatz, including the  $k$ -UpCCGSD method developed by Lee *et al*[23]. and the ADAPT-VQE algorithm proposed by Grimsley *et al*[24].

In this article, we proposed an alternative method on the basis of the unitary coupled-cluster ansatz. First, the contribution of each cluster operator is measured and sorted on the top of the Hartree-Fock reference (HF) state. The terms that lead to energy reduction over a pre-defined threshold are picked out in order to form a new operator pool. Then, the new pool is used to generate an approximated wave function. Additional operators are added into the new operator pool based on the sorted sequence in the first step and grows the ansatz iteratively. We term the above algorithm as energy-sorting (ES) algorithm. The main difference of ES algorithm from ADAPT-VQE is that we use a single-shot evaluation to "score" each operator at the very beginning, and the overhead of measurements will not be significantly increased during the growth of the wave function ansatz.

\* [ywl0s@163.com](mailto:ywl0s@163.com)

† [yung.manhong@huawei.com](mailto:yung.manhong@huawei.com)

Our benchmark results show that the ES algorithm is able to retain the accuracy of the original UCCSD in a couple of iterations. With a more robust operator pool such as UCC with generalized singles and doubles (UC-CGSD), the ES algorithm is able to reach chemical accuracy for strongly correlated system such as  $H_6$  molecule. The number of operators is reduced dramatically by a factor up to 14 after the ES optimization, thus effectively reduce the depth of quantum circuit. Our algorithm is able to capture the dominant operator terms and greatly reduce quantum resources overhead compare to the conventional UCCSD method, making it promising in quantum chemistry simulations on NISQ device.

The rest parts of the paper are organized as follows. We begin with a brief review of the VQE algorithm and the UCC ansatz in Sec.IIA. In Sec.IIB we give a detailed description of the energy-sorting algorithm. A schematic flowchart is presented to illustrate the implementation of ES algorithm for quantum chemistry simulations. In Sec.III the benchmark results of the ES algorithm are given for chemical systems including  $H_4$ ,  $LiH$ ,  $H_6$  and the periodic one-dimensional (1D) hydrogen chain. Finally, we conclude our work and provide suggestions for further improvements of the algorithm.

## II. METHOD

### A. Ground-state ansatz

The second-quantized formulation of quantum chemistry leads to the Hamiltonian under Born-Oppenheimer approximation as

$$\hat{H} = \sum_{p,q} h_{pq} a_p^\dagger a_q + \sum_{p,q,r,s} \frac{1}{2} h_{rs}^{pq} a_p^\dagger a_q^\dagger a_r a_s \quad (1)$$

where  $a_i^\dagger$  and  $a_j$  are Fermionic creation and annihilation operators, and the one-body and two-body coefficients  $h_{pq}$  and  $h_{rs}^{pq}$  in Eq.(1) can be computed on the classical computer. The ground-state wave function and energy is then solved from the eigenvalue problem

$$\hat{H}|\Psi\rangle = E|\Psi\rangle \quad (2)$$

In the VQE algorithm, the key ingredient is the parametric unitary operator to prepare the wave function ansatz

$$|\Psi(\vec{\theta})\rangle = U(\vec{\theta})|\Psi_0\rangle, \quad (3)$$

where the reference wave function  $|\Psi_0\rangle$  is usually chosen to be the Hartree-Fock state. The parametric wave function is then optimized according to Rayleigh-Ritz variational principle

$$E = \min_{\vec{\theta}} \langle \Psi(\vec{\theta}) | \hat{H} | \Psi(\vec{\theta}) \rangle \quad (4)$$

In a typical VQE framework, chemical and physical quantities, for example, total energy of the system, are

evaluated on a quantum computer. The gradients can be obtain through finite difference steps or using the parameter-shift rule. The optimization of parameters are then performed on a classic computer using conventional optimizer such as Conjugated-Gradient or Simultaneous Perturbation Stochastic Approximation or Nelder-Mead.

The unitary coupled-cluster[25–27] (UCC) ansatz is one of the most commonly used PMA ansatz in electronic structure simulations. Unlike the traditional coupled-cluster theory, the energy and wave function under UCC are determined variationally using Eq.(4). The unitary operator  $U(\vec{\theta})$  is defined as

$$|\Psi\rangle = \exp(\hat{T} - \hat{T}^\dagger)|\Psi_0\rangle, \quad (5)$$

where  $|\Psi_0\rangle$  is chosen to be the single-determinant Hartree-Fock (HF) wave function. The cluster operator that truncated at single- and double-excitations has the form of

$$T(\vec{\theta}) = \sum_{p,q}^{p \in vir, q \in occ} \theta_q^p \hat{T}_q^p + \sum_{p>q, r>s}^{p,q \in vir, r,s \in occ} \theta_{rs}^{pq} \hat{T}_{rs}^{pq} \quad (6)$$

where the one- and two-body terms are defined as

$$\hat{T}_q^p = a_p^\dagger a_q \quad (7)$$

$$\hat{T}_{rs}^{pq} = a_p^\dagger a_q^\dagger a_r a_s \quad (8)$$

Using Fermion-to-Qubit transformations such as Jordan-Wigner or Bravyi-Kitaev[28–31], the unitary operator  $U(\vec{\theta}) = \exp(\hat{T} - \hat{T}^\dagger)$  can then be written as:

$$U(\vec{\theta}) = \exp(i \sum_{p,\alpha} \tilde{\theta}_p^\alpha \sigma_p^\alpha + i \sum_{pq,\alpha\beta} \tilde{\theta}_{pq}^{\alpha\beta} \sigma_p^\alpha \sigma_q^\beta + \dots) \quad (9)$$

$$\hat{H} = \sum_{p,\alpha} h_p^\alpha \sigma_p^\alpha + \sum_{pq,\alpha\beta} h_{pq}^{\alpha\beta} \sigma_p^\alpha \sigma_q^\beta + \dots \quad (10)$$

where  $\sigma_p^\alpha, \sigma_q^\beta \in \{\sigma_x, \sigma_y, \sigma_z, I\}^\otimes$  and  $p, q, \dots$  are indices of qubits, where  $\{\tilde{\theta}\}$  and  $\{\theta\}$  span the same parameter space.

On a quantum computer, the implementation of the VQE circuit for UCCSD ansatz requires decomposition of the exponential-formed cluster operators into basic quantum single-qubit and two-qubit gates. Approximation schemes are often used, such as Trotter-Suzuki decomposition[32, 33]:

$$\exp(\hat{A} + \hat{B}) = \lim_{N \rightarrow \infty} (e^{(\hat{A}/N)} e^{(\hat{B}/N)})^N \quad (11)$$

The Trotterized UCC wave function takes the form:

$$|\Psi\rangle = \prod_{k=1}^N \prod_{i=1}^{N_i} e^{\frac{\theta_i}{N} \hat{\tau}_i} |\Psi_0\rangle, \quad (12)$$

where  $N_i$  is the total number of individual operators  $\hat{\tau}_i$ . The Trotterization is truncated at finite order  $N$ , and the number of Trotter steps, the ordering sequence of operators and the Trotter formula used in the procedure will have significant influence on the accuracy of the simulation. In this study, we use the single-step Trotter decomposition. Here, we summarize the procedure of the VQE method with unitary coupled-cluster ansatz (UCC-VQE) in **Algorithm 1**

**Algorithm 1:** Procedure of VQE algorithm for UCC ansatz

---

**Input:**  
 Reference state  $|\Psi_0\rangle$  (such as  $|\Psi_{HF}\rangle$ )  
 System Hamiltonian  $\hat{H}$

**Output:**  
 The optimized ansatz and energy

- 1 Prepare initial wave function;
- 2 Generate parametric cluster operators and map the unitary cluster operators to quantum circuit; **while** not converged, i.e.  $\Delta E^{(k)} \geq \varepsilon$  **do**
- 3 Measure multiple times to obtain the expectation of  $E^{(k)} = \langle \Psi(\vec{\theta}^{(k)}) | \hat{H} | \Psi(\vec{\theta}^{(k)}) \rangle$ ;
- 4 Perform classical optimization algorithm to update parameters:  $\vec{\theta}^{(k)} \rightarrow \vec{\theta}^{(k+1)}$ ;
- 5 Update quantum circuit for the next iteration
- 6 **end**

---

## B. Energy-sorting VQE algorithm

VQE significantly relieves the hardware demand compared to QPE. However, the trading in long circuit depth is achieved at the expense of a much higher number of measurements. Our proposed energy-sorting algorithm would require circuits with much shallower depth and reduced number of measurements dramatically, by selecting only the important terms in the original operator pool. We name this protocol as the ES-VQE method.

As a typical post-Hartree-Fock method, the coupled-cluster (CC) wave function is treated as an exponential of the cluster operators on a reference state:

$$|\Psi\rangle = \exp(\hat{T})|\Psi_0\rangle \quad (13)$$

Expanding the exponential formalism, we can simply write the CC energy as:

$$\begin{aligned} E &= \langle \Psi_0 | e^{-\hat{T}} | \hat{H} | e^{\hat{T}} | \Psi_0 \rangle \\ &\approx \langle \Psi_0 | \hat{H} | \Psi_0 \rangle + \sum_{i,j} t_{ij} \langle \Psi_i | \hat{H} | \Psi_j \rangle \end{aligned} \quad (14)$$

Due to the exponential ansatz, CC can implicitly include higher excitation operators, leading to fast convergence behaviour.

For UCCSD, a similar expansion of energy can be obtained by replacing  $\hat{T}$  with  $\hat{T} - \hat{T}^\dagger$ . In general, the total

energy can be expressed as the Hartree-Fock energy  $E_0 = \langle \Psi_0 | \hat{H} | \Psi_0 \rangle$  plus the correlation part  $\sum t_{ij} \langle \Psi_i | \hat{H} | \Psi_j \rangle$ . Each cluster operator contributes a part of the correlation energy. However, their contributions are not necessarily equal, for example, excitations near the highest occupied orbitals (HOMO) or lowest unoccupied orbitals (LUMO) may have larger contributions. Based on this idea, by adding operators according to their "importance", a compact optimal wave function ansatz based on UCCSD is thus constructed. A detailed explanation of the ES-VQE algorithm used in this work is given in Appendix.(A).

The basic outline of ES-VQE is drawn schematically in Fig.(1). Here we described the ES-VQE method as follows:

- 1) Initialize the qubits or quantum register, and prepare the reference state. In this work, we use the Hartree-Fock state as the reference state. The quantities such as one- and two-electron integrals for preparing the initial input is calculated on a classical computer.
- 2) Define an operator pool  $\mathcal{O}$  to build the wave function ansatz, for example, UCCSD operator pool. The operator pool contains all the terms which may be used to generate the wave function ansatz.
- 3) On a quantum computer, perform VQE optimization iterations for each operator  $\hat{\tau}_i \in \mathcal{O}$ . This can be carried out in parallel if multiple quantum processors are available. Evaluate the energy  $E_i$  optimized by using only a single cluster operator  $\hat{\tau}_i$  and calculate its difference relative to the reference state:  $\Delta E_i = E_i - E_{HF}$ . Record and form a sorted list  $\mathcal{E} = \{(\Delta E_i, \hat{\tau}_i)\}_{sorted}$  in descending order of  $\Delta E_i$ .
- 4) The first iteration starts with a subset of operators from the original pool. Select operators  $\{\hat{\tau}_i\}$  with total energy contribution above a threshold  $\Delta E_i > \varepsilon$ . Perform VQE to optimized parameters in the generated ansatz.
- 5) Select next one or more operators from the sorted list  $\mathcal{E}$ . The wave function ansatz is then updated using the selected terms on top of the previous chosen operators. VQE is performed again and re-optimize all the parameters. Denote the energy and wave function at the  $(k)$ th ( $k \geq 1$ ) iteration as  $E^{(k)}$  and  $|\Psi^{(k)}\rangle$ . If the absolute difference in energy of the  $k$ th and  $(k+1)$ th iteration is larger than some threshold  $\tilde{\varepsilon}$ , accept the ansatz  $|\Psi^{(k+1)}\rangle$ .
- 6) If some convergence criteria is satisfied, for example, reaches chemical accuracy, then output the optimized wave function  $|\Psi^{opt}\rangle$  together with corresponding energy  $E^{opt}$  and exit, otherwise re-run step 5.

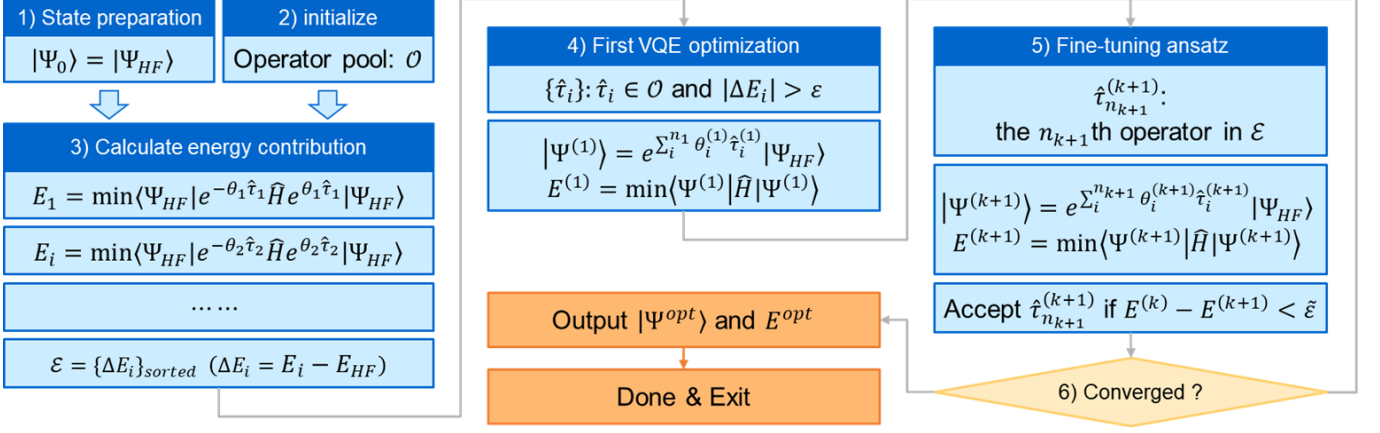


FIG. 1. Procedure of the optimized UCC-VQE scheme. Before the first iteration, the energy contribution  $\mathcal{E} = \{\Delta E_i\}$  of each operator  $\hat{\tau} \in \mathcal{O}$  is calculated and sorted through a short VQE circuit. At each iteration, one or more operators are selected from the initial operator pool  $\mathcal{O}$  according to the sorted sequence in  $\mathcal{E}$ . The wave function ansatz grows step-by-step until some convergence criteria is reached.

As described above and in Fig.(1), at the beginning of ES-VQE algorithm, an additional loop of VQE will be performed to estimate the influence of each operator on the total energy:

$$E_i = \min_{\theta_i} \langle \Psi_HF | e^{-\theta_i \hat{\tau}_i} \hat{H} e^{\theta_i \hat{\tau}_i} | \Psi_HF \rangle \quad (15)$$

The result  $\Delta E_i = E_i - E_{HF}$  is then stored and sorted in a list, namely  $\mathcal{E}$  on the classical computer. The next iterations will take the excitation operators following the order in  $\mathcal{E}$ . At the first iteration, all the operators  $\hat{\tau}_i$  with  $\Delta E_i$  larger than a given threshold  $\varepsilon$  will be used to construct a wave function ansatz which is an approximation to the unknown ground state. It should be point out that the summation of  $\Delta E_i$  is often not exactly equal to the correlation energy computed using UCCSD due to the Trotterization decomposition:

$$\sum_i^N \Delta E_i \neq \langle \Psi(\vec{\theta}_{opt}) | \hat{H} | \Psi(\vec{\theta}_{opt}) \rangle - E_{HF} \quad (16)$$

where  $\Psi(\vec{\theta}_{opt})$  is the converged UCCSD wave function and  $\vec{\theta}_{opt}$  is the optimized parameters. Therefore, selecting more operators in step 4 with a very small  $\varepsilon \rightarrow 0$  may not be an optimal option. Usually the threshold  $\varepsilon$  will be set to the value of a 2-3 orders of magnitude smaller than the chemical accuracy. If this pool with the above threshold fail to converge to the ground-state energy, extra iterations might be needed which is described in step 5. In step 5, starting from the 2nd iteration, the ansatz is growing by adding one or more terms corresponding to the next few largest  $\Delta E_i$ s in the sorted list  $\mathcal{E}$  and re-optimizing all the parameters. Note that for different reference states, for example,  $|\Psi^{(k)}\rangle$  and  $|\Psi^{(k+1)}\rangle$ , the contributions of a single operator  $\hat{\tau}_i$  to the total energy in the Trotterized wave function  $e^{\theta_i \hat{\tau}_i} |\Psi^{(k)}\rangle$

and  $e^{\theta_i \hat{\tau}_i} |\Psi^{(k+1)}\rangle$  may not be the same, therefore step 6 is necessary to ensure that all or most of the operators used in the final ansatz have non-zero amplitudes.

### III. RESULTS

We demonstrate our method for both non-periodic(molecules) and periodic systems. The benchmarks are performed using a in-house developed code to perform the ES-VQE algorithm. The one- and two-body integrals are calculated using the PySCF software[34]. The mapping from Fermion operators to qubit representations are obtained by Jordan-Wigner transformation using MindQuantum[35]. The gradient-based optimization is performed utilizing the Broyden-Fletcher-Goldfarb-Shannon (BFGS) algorithm which is implemented in the SciPy package[36] with convergence criteria  $gtol=10^{-7}$  a.u. The wave function ansatz constructed through UCC-VQE and ES-VQE involves single-step Trotter-Suzuki decomposition. The operator selection threshold  $\varepsilon$  in **Algorithm 1 step 4** and the energy threshold  $\tilde{\varepsilon}$  in **step 6** are chosen to be  $1 \times 10^{-4}$  Hartree and  $1 \times 10^{-8}$  Hartree respectively. The convergence criteria is defined as

$$(E^{(k)} - E_{FCI} < \varepsilon_c) \quad || \quad (k > N_{op}) \quad (17)$$

where  $\varepsilon_c = 1.0$  kcal/mol ( $1.6 \times 10^{-3}$  Hartree) stands for chemical accuracy and  $N_{op}$  is the total number of operators in the operator pool  $\mathcal{O}$ .  $E_{FCI}$  represents energy obtained through full configuration interaction. Note that in some cases the UCCSD operator pool is not able to generate the ansatz with energy difference from FCI less than  $1.6 \times 10^{-3}$  Hartree, therefore the second criteria  $k > N_{op}$  will terminate the algorithm if all the operators in the pool  $\mathcal{O}$  have been traversed. ES-VQE with

UCCSD operator pool is named as ES-UCCSD-VQE. Operator pool generated from UCC with generalized singles and doubles (UCCGSD)[23, 37–39] is also used (ES-UCCGSD-VQE).

For non-periodic systems, three molecules  $H_4$ ,  $LiH$  and  $H_6$  are tested. The minimum STO-3G basis set is used for the calculations. The calculated potential energy surface as a function of nuclear coordinates are shown in Fig.(2), together with error with respect to the FCI energy and the number of operators used in the final wave function ansatz. Results of HF and UCCSD are compared with ES-UCCSD-VQE/ES-UCCGSD-VQE. In general, ES-UCCSD-VQE successfully maintains the accuracy comparable to original UCCSD using the complete operator pool, meanwhile significantly reduces the number of variational parameters. For  $H_4$  we obtain a factor of 2.7 to 3.7 in the reduction in number of operators. For  $H_6$  which have more significant strongly-correlated effect, a reduction factor of 2.8 to 3.2 is observed. While for weakly-correlated systems such as  $LiH$ , a greater reduction factor ranging from 3.6 to 14 is obtained, especially at shorter  $Li-H$  distance. As the UCCGSD operator pool is introduced, chemical accuracy (error within  $1.6 \times 10^{-3}$  Hartree with respect to the FCI energy) is achieved throughout the potential energy curve for all three tested molecules. Since the iterations of ES-VQE algorithm used in the benchmark will stop if chemical accuracy is reached according to Eq.(17), it can be expected that the error of ES-VQE from FCI will be improved if more strict convergence criteria is set.

We also test our algorithm for the periodic one-dimensional hydrogen chain. We use the SVZ basis set together with GTH pseudopotential[40]. The unit cell consists of two hydrogen atoms. Three  $k$ -points are sampled along the chain, making a total number of 12 qubits in the simulation. Quantum simulations for periodic systems can be challenging and may faced with both accuracy and resource issues due to the residual error introduced by complex wave function and the necessity for dense  $k$ -point sampling grid. Our previous work[41, 42] pointed out that the original implementation of the unitary coupled-cluster method failed to give accurate prediction of ground states in periodic systems, and a complementary operator pool is necessary to achieve accurate ground state energy:

$$\tilde{\tau}_q^p = i(a_p^\dagger a_q + a_q^\dagger a_p) \quad (18)$$

$$\tilde{\tau}_{rs}^{pq} = i(a_p^\dagger a_q^\dagger a_r a_s + a_s^\dagger a_r^\dagger a_q a_p) \quad (19)$$

More details about the residual error is presented in Appendix.(B).

The benchmark results for 1D hydrogen chain are presented in Fig.(3). The FCI results used for benchmark are obtained by directly diagonalizing the Hamiltonian. Similar to  $H_4$  and  $H_6$ , although ES-UCCSD-VQE successfully reaches the chemical accuracy of UCCSD, the UCCSD itself is not able to provide chemical accuracy

across the potential energy surface with all the single- and double-excitation operators traversed. We observe that using the UCCGSD operator pool, ES-UCCGSD-VQE greatly suppressed the error to below chemical accuracy at the expense of a few more operators, which is in agreement with previous studies that UCCGSD provides more stable and accurate ground-state predictions not only in molecular calculations but also in periodic systems[23, 41]. By identifying and gathering the dominant excitations which have large contributions to total energy, ES-UCCSD-VQE algorithm shows excellent performance for the 1D hydrogen chain, by selecting only 20 percent of the operators from the original UCCSD pool. As for ES-UCCGSD-VQE, although more terms are required to reach chemical accuracy at larger  $H-H$  distance, the reduction in the number of operators is still remarkable, with a factor of 14 (26 out of 360 UCCGSD operators). Applications in larger periodic systems are therefore promising.

It is worthy noting that at step 5 of the ES-VQE algorithm, the number of parameters to be re-optimized contains  $n_{k+1}$  terms, where  $n_{k+1}$  is the number of operators used at the  $(k+1)th$  iteration. We note that for the same term  $\hat{\tau}_{i_0}$ , the optimized value of its coefficient between different iterations  $k_1$  and  $k_2$  are generally different. An alternative optimization scheme is tested by freezing the previously optimized  $n_k$  parameters while only optimized the newly added terms. Unfortunately, deterioration in both number of operators and accuracy is observed. The results are shown in Appendix.(C)

#### IV. CONCLUSION

In this work, we proposed an optimized energy-sorting algorithm named ES-VQE to build the wave function ansatz. With this algorithm, effective excitation operators are identified to form an ordered sequence. The wave function ansatz is then constructed using this in-order operator pool. ES-VQE successfully achieved UCCSD accuracy for both non-periodic and periodic systems, with up to 14 times reduction in term of operator pool size, thus effectively reduces the quantum circuit depth and the number of measurements. By using a more robust operator pool such as UCCGSD[23, 41], ES-VQE shows the ability to achieve higher precision of the ground-state energy at the expense of a few more operators. Our algorithm shows a potential of huge resource reduction while preserving the simulation accuracy, paving the way toward efficiently simulating larger chemical systems on near-term quantum computers.

To make the ES-VQE algorithm more suitable for the NISQ device, quantum circuit compilation and optimization that consider hardware constraints is needed to further suppress the circuit depth. Besides, efficient measurement scheme is also required in order to reduce the overhead of measurements. By combining the ES-VQE algorithm with other methods such as parameter reduc-

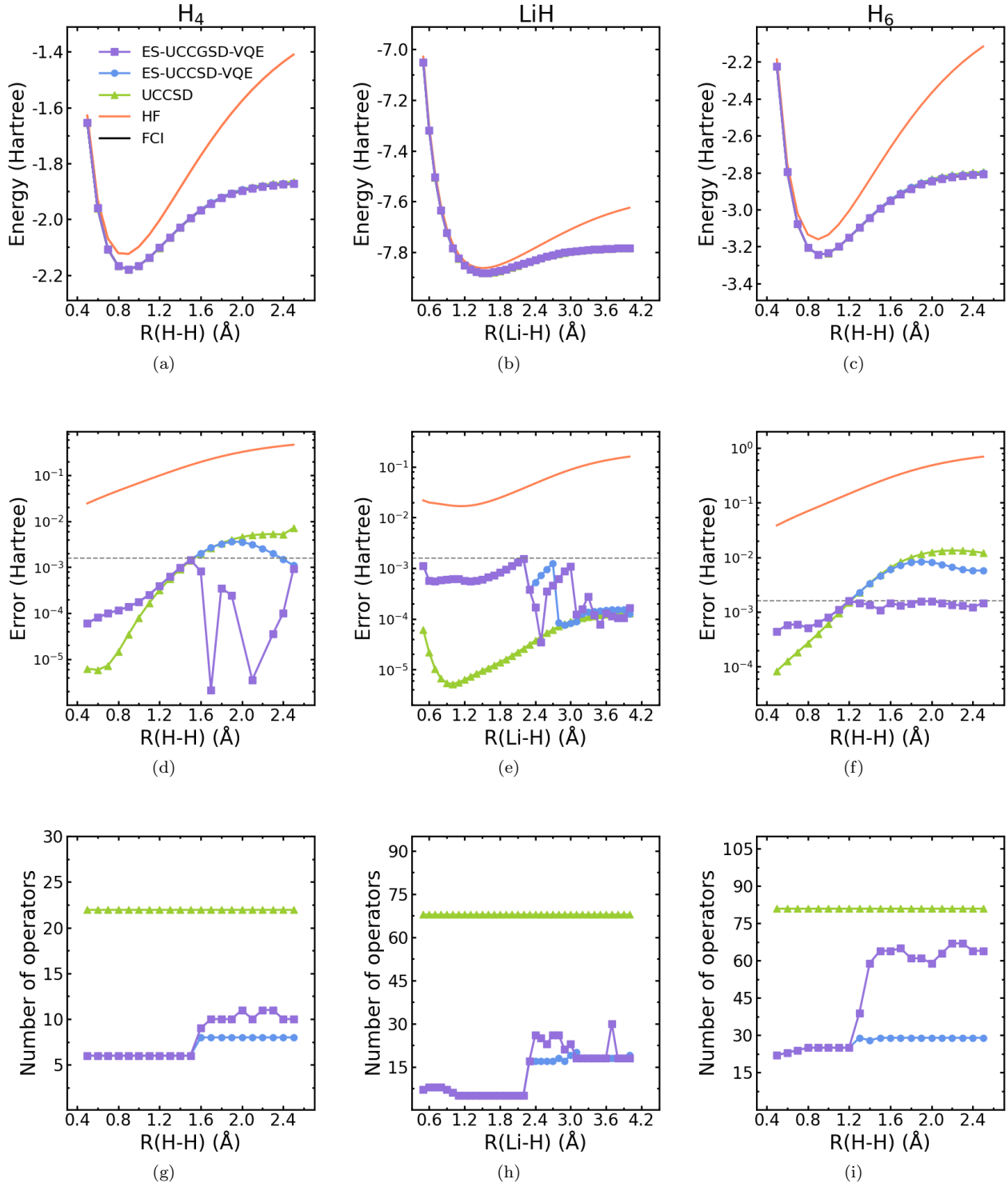


FIG. 2. The calculated results for  $H_4$ ,  $LiH$  and  $H_6$ . (a,b,c). Potential energy surface calculated using ES-UCCSD-VQE/ES-UCCGSD-VQE in atomic units (Hartree). (d,e,f). Absolute error in energy of different method with respect to FCI, unit in Hartree. The dashed lines indicate chemical accuracy at  $1.6 \times 10^{-3}$  Hartree. The energy error is plotted using logarithmic axis. (g,h,i). Number of operators in the final ansatz optimized by ES-UCCSD-VQE/ES-UCCGSD-VQE.

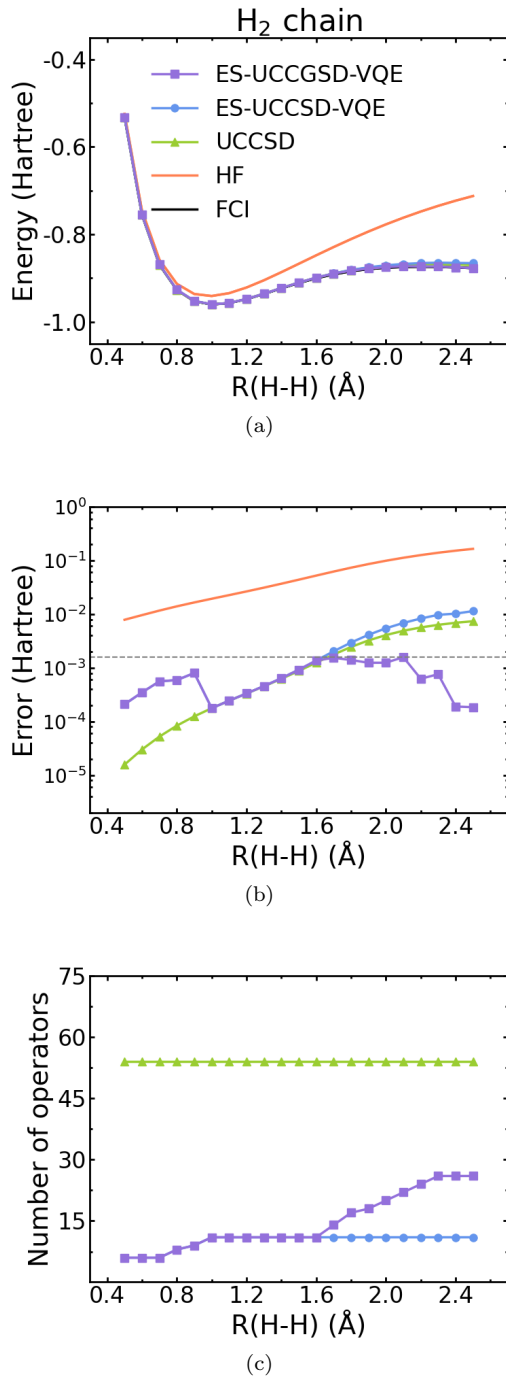


FIG. 3. The benchmark results of ES-UCCSD-VQE and ES-UCCGSD-VQE for 1D equispaced hydrogen chain. Two atoms per primitive cell with three sampled  $k$ -points are used in the calculation. An extended operator pool with auxiliary terms defined by Eq.(18)-(19) is used in order to minimize the residual error from complex wave functions. (a). Potential energy curve in unit Hartree of 1D hydrogen chain as a function of H-H distance. (b). Deviation of energy calculated by different methods from FCI results in logarithmic axis. (c). Total number of terms in the final ansatz.

tion techniques considering point-group symmetry, effi-

cient large-scale simulations for both molecular and periodic systems can be performed on NISQ devices.

### Appendix A: Identifying the effective operators

The state ansatz used in VQE can be expressed as,

$$|\Psi(\vec{\theta})\rangle = U(\vec{\theta})|\Psi_{HF}\rangle \quad (A1)$$

where the reference state is taken as the Hartree-Fock state. Moreover,  $U(\vec{\theta})$  is a parametric unitary operator, which can be expressed as,

$$U(\vec{\theta}) = \exp(M(\vec{\theta})) \quad (A2)$$

Suppose we separate  $M$  into the dominant part  $M^{(0)}$  and a correction part  $M'$ , i.e.,

$$U(\vec{\theta}) = \exp(M^{(0)} + M') , \quad (A3)$$

where  $M'$  (under certain expansion) may contain multiple terms, for example,  $M' = M^{(1)} + M^{(2)} + \dots$ . The total energy  $E$  can be decomposed into a similar form:

$$E(\vec{\theta}) = E^{(0)} + E' \quad (A4)$$

where  $E' = E^{(1)} + E^{(2)} + \dots$  and  $E^{(i)} \ll E^{(j)}$  if  $i < j$ . Under the Trotter-Suzuki decomposition, the wave function ansatz takes the form:

$$|\Psi\rangle = \prod_i \exp(M^{(i)})|\Psi_{HF}\rangle \quad (A5)$$

If we ignore all  $M' \equiv \mathbf{0}$ , then an zeroth-order approximation to the ground state is obtained:

$$\hat{H} \exp(M^{(0)})|\Psi_{HF}\rangle = E^{(0)} \exp(M^{(0)})|\Psi_{HF}\rangle \quad (A6)$$

Denote  $\exp(M^{(0)})|\Psi_{HF}\rangle$  as  $|\Psi^{(0)}\rangle$ , and add  $M^{(1)}$  into the zeroth-order ansatz, we have:

$$\hat{H} \exp(M^{(1)})|\Psi^{(0)}\rangle = E^{1st} \exp(M^{(1)})|\Psi^{(0)}\rangle \quad (A7)$$

where  $E^{1st} = E^{(0)} + E^{(1)}$ . Multiply  $\exp(M^{(1)})$  on the left of Eq.(A6):

$$\begin{aligned} \exp(M^{(1)})\hat{H}|\Psi^{(0)}\rangle &= \exp(M^{(1)})E^{(0)}|\Psi^{(0)}\rangle \\ &= E^{(0)}\exp(M^{(1)})|\Psi^{(0)}\rangle \end{aligned} \quad (A8)$$

Subtract Eq.(A7) and Eq.(A8),

$$[\hat{H}, \exp(M^{(1)})]|\Psi^{(0)}\rangle = E^{(1)} \exp(M^{(1)})|\Psi^{(0)}\rangle \quad (A9)$$

Our goal is to find  $M'$  such that  $E^{(1)}$  is minimized. This can be done through a minimization procedure:

$$E^{(1)} = \min_{M^{(1)}} \{ \langle \Psi^{(0)} | [\hat{H}, \exp(M^{(1)})] | \Psi^{(0)} \rangle \} . \quad (A10)$$

For  $M^{(i)}$  ( $i \geq 1$ ), similar procedures can be carried out using Eq.(A7)-(A10). It should be noted that  $M^{(i)}$  may

contain not only the variational parameters  $\{\theta\}$  but also tensor products of different combinations of operators  $\{\hat{\tau}\}$  taken from some operator pool  $\mathcal{O}$ . The minimization should run over all possible combinations of  $\hat{\tau}_i \in \mathcal{O}$  using a loop-structured procedure, and the optimization of parameters  $\{\theta\}$  can be done using VQE.

Notice that the above optimization in the space spanned by the operator pool is not a trivial work. The global optimal selection requires an exponentially large number of trials. In this work, we choose  $M^{(i)}$  such that it contains only the single term  $\hat{\tau}_{i_0} \in \mathcal{O}$ . By setting  $M^{(0)} \equiv \mathbf{0}$ , Eq.(A10) reduces to searching for the suitable initial approximation  $M^{(0)}$  for Eq.(A6), and the minimization procedure is equivalent to the step 3 described in the ES-VQE algorithm.

## Appendix B: Residual error in the UCC ansatz for periodic systems

The anti-Hermitian contracted Schrödinger equation described the convergence criteria as[41, 43]:

$$\langle \Psi | [\hat{T}_u, \hat{H}] | \Psi \rangle = 0 \quad (B1)$$

where  $\hat{T}_u$  is a general two-body operator. Eq.(B1) can be separated into the summation of real (ACSE-Re) and imaginary (ACSE-Im) part:

$$\langle \Psi | [\hat{T}_u - \hat{T}_u^\dagger, \hat{H}] | \Psi \rangle = 0 \quad (B2)$$

$$\langle \Psi | [\hat{T}_u + \hat{T}_u^\dagger, \hat{H}] | \Psi \rangle = 0 \quad (B3)$$

The convergence condition of Trotterized UCC-VQE with real-valued parameters is equivalent to the real part Eq.(B2) of the anti-Hermitian CSE. For the imaginary part, although it is not directly optimized during VQE, non-periodic systems with real-valued wave function ensures its value to be constantly zero.

As the complex-valued wave function is used for periodic systems, the residual error, which refers to the imaginary part of anti-Hermitian CSE in Eq.(B3), will have non-zero values and not guarantee to be minimized through VQE procedure. Our previous study[41] shows that in the final ansatz, the residual error can be larger than  $8 \times 10^{-3}$  Hartree. One solution is to use the K2G transformation[41], which transforms the complex HF orbitals to real-valued wave function for a  $\Gamma$ -centered supercell. Another solution employs complex-valued variational parameters and separately optimizing the real and imaginary parts, as studied by Manrique *et al.*[44]. We used an alternative method by adding the terms in Eq.(B3) back into the unitary coupled-cluster ansatz as a auxiliary operator pool, shown as Eq.(18) and Eq.(19).

## Appendix C: Optimization scheme

An alternative approach to perform VQE optimization is to treat the wave function ansatz at  $(k+1)th$  iteration

as:

$$|\Psi^{(k+1)}\rangle = \exp(\theta_{n_{k+1}}^{(k+1)} \hat{\tau}_{n_{k+1}}) \prod_i^{n_k} \exp(\theta_i^{(k)} \hat{\tau}_i) |\Psi_{HF}\rangle \quad (C1)$$

where  $|\Psi^{(k)}\rangle$  is the optimized ansatz of the previous iteration. The original optimization scheme, namely full-parameter optimization, optimizes all  $n_{k+1}$  parameters simultaneously. However, in the single-parameter optimization strategy, the first  $n_k$  amplitudes will be kept fixed during the VQE procedure. In order to show the difference between these two methods clearly, we choose the periodic 1D hydrogen chain with distance between two hydrogen atoms in the unit cell  $R(H-H)=2.0 \text{ \AA}$  as an example. The UCCGSD operator pool is used here to minimize the possible error introduced by the UCCSD pool. The convergence criteria is unchanged, as in Eq.(17).

ES-UCCGSD-VQE	$\Delta E_{abs}$ (Hartree)	$N_{ops}$
Full-parameter	$1.25 \times 10^{-3}$	20
Single-parameter	$3.63 \times 10^{-3}$	360

TABLE I. Results of different optimization schemes used in step 5 of ES-VQE. For full-parameter optimization, all  $n_{k+1}$  parameters are optimized simultaneously at the  $(k+1)th$  iteration. Single-parameter strategy only update the coefficient of the newly added term while frozen other values. The test is performed using 1D hydrogen chain at  $R(H-H)=2.0 \text{ \AA}$  and UCCGSD supplied operator pool.

Table.(I) listed the results of two different optimization strategies. Using the UCCGSD operator pool, ES-UCCGSD-VQE successfully reaches chemical accuracy with 20 operators selected from 360 operators. However, for the single-parameter update scheme, we fail to obtain the ground state energy with chemical accuracy even with all the 360 operators. This is due to the fact that single-parameter update scheme limits the optimization to a local minimum near the previous state. The partial derivative  $\partial E(\vec{\theta})/\partial \theta_j$  is correlated with other terms  $\{\theta_i \mid i \neq j\}$ . Therefore, updating only the last parameter will be unable to find the correct minimum in the parameter space spanned by  $\{\theta_i^{(k+1)} \mid i = 1 \dots n_{k+1}\}$ .

## Appendix D: $k$ -point sampling scheme

In calculations of periodic systems, a finite number of  $k$ -points are required to sample the Brillouin zone. In this work, we used a gamma-centered Monkhorst-Pack scheme[45] for generating  $k$ -points for the 1D equispaced hydrogen chain. A Monkhorst-Pack grid is a rectangular grid of points sampled evenly throughout the first Brillouin zone with dimension  $N_{k_x} \times N_{k_y} \times N_{k_z}$ .

Take the 1D hydrogen chain with H-H distance 1.0  $\text{\AA}$  and three sampled  $k$ -points as an example:

1) The unit cell can be represented by a 3-dimensional matrix:

$$R = \begin{bmatrix} \mathbf{a}_1 \\ \mathbf{a}_2 \\ \mathbf{a}_3 \end{bmatrix} = \begin{bmatrix} 10.0 & 0.0 & 0.0 \\ 0.0 & 10.0 & 0.0 \\ 0.0 & 0.0 & 2.0 \end{bmatrix} \quad (\text{D1})$$

Two hydrogen atoms are aligned along  $z$ -axis (the direction of  $\mathbf{a}_3$ ).

2) The reciprocal lattice vectors  $\{\mathbf{b}_1, \mathbf{b}_2, \mathbf{b}_3\}$  can be calculated using:

$$\mathbf{b}_1 = 2\pi \frac{\mathbf{a}_2 \times \mathbf{a}_3}{\mathbf{a}_1 \cdot (\mathbf{a}_2 \times \mathbf{a}_3)} \quad (\text{D2})$$

$$\mathbf{b}_2 = 2\pi \frac{\mathbf{a}_3 \times \mathbf{a}_1}{\mathbf{a}_2 \cdot (\mathbf{a}_3 \times \mathbf{a}_1)} \quad (\text{D3})$$

$$\mathbf{b}_3 = 2\pi \frac{\mathbf{a}_1 \times \mathbf{a}_2}{\mathbf{a}_3 \cdot (\mathbf{a}_1 \times \mathbf{a}_2)} \quad (\text{D4})$$

which is equivalent to

$$G = \begin{bmatrix} \mathbf{b}_1 \\ \mathbf{b}_2 \\ \mathbf{b}_3 \end{bmatrix} = 2\pi \cdot (R^T)^{-1} \quad (\text{D5})$$

Therefore, the reciprocal lattice vectors in this example is obtained using Eq.(D2)-(D5) ( $\text{\AA}^{-1}$ ):

$$G = \begin{bmatrix} 0.6283 & 0.0 & 0.0 \\ 0.0 & 0.6283 & 0.0 \\ 0.0 & 0.0 & 3.1416 \end{bmatrix} \quad (\text{D6})$$

3) For a  $1 \times 1 \times 3$  grid, the coordinates for the sampled  $k$ -points are thus ( $\text{\AA}^{-1}$ ):

$$\vec{K}_1 = \frac{0}{3} \cdot \mathbf{b}_3 = (0.0, 0.0, 0.0) \quad (\text{D7})$$

$$\vec{K}_2 = \frac{1}{3} \cdot \mathbf{b}_3 = (0.0, 0.0, 1.0472) \quad (\text{D8})$$

$$\vec{K}_3 = -\frac{1}{3} \cdot \mathbf{b}_3 = (0.0, 0.0, -1.0472) \quad (\text{D9})$$

Bloch atomic orbitals are then defined as:

$$\chi_{\mu\vec{K}}(\vec{r}) = \frac{1}{\sqrt{N}} \sum_{\vec{R}_n} e^{i\vec{K}\cdot\vec{R}_n} \chi_{\mu}(\vec{r} - \vec{R}_n) \quad (\text{D10})$$

where  $\chi_{\mu}$  is some atom-centered basis function,  $\vec{K}$  is a crystal momentum vector similar to Eq.(D7-D9), and  $N$  is the total number of unit cells. Using linear combination of atomic orbitals (LCAO), the periodic HF orbitals can be expressed as:

$$\phi_{p\vec{K}}(\vec{r}) = \sum_{\mu} C_{\mu p}(\vec{K}) \chi_{\mu\vec{K}}(\vec{r}) \quad (\text{D11})$$

The corresponding eigenvalue equation at each  $\vec{K}$  is therefore given by:

$$F(\vec{K})C(\vec{K}) = S(\vec{K})C(\vec{K})E(\vec{K}), \quad (\text{D12})$$

where the elements of Fock matrix  $F$  and overlap matrix  $S$  are given by:

$$F_{\mu\nu}(\vec{K}) = T_{\mu\nu}(\vec{K}) + V_{\mu\nu}^{pp}(\vec{K}) + J_{\mu\nu}(\vec{K}) - K_{\mu\nu}(\vec{K}) \quad (\text{D13})$$

$$T_{\mu\nu}(\vec{K}) = -\frac{1}{2} \int_{\Omega} \chi_{\mu\vec{K}}^*(\vec{r}) \nabla_{\vec{r}}^2 \chi_{\nu\vec{K}}(\vec{r}) d\vec{r} \quad (\text{D14})$$

$$J_{\mu\nu}(\vec{K}) = \int \int_{\Omega} \chi_{\mu\vec{K}}(\vec{r}) \frac{\rho(\vec{r}, \vec{r}')}{|\vec{r} - \vec{r}'|} \chi_{\nu\vec{K}}^*(\vec{r}') d\vec{r} d\vec{r}' \quad (\text{D15})$$

$$K_{\mu\nu}(\vec{K}) = \int \int_{\Omega} \chi_{\mu\vec{K}}(\vec{r}) \frac{\rho(\vec{r}, \vec{r}')}{|\vec{r} - \vec{r}'|} \chi_{\nu\vec{K}}^*(\vec{r}') d\vec{r} d\vec{r}' \quad (\text{D16})$$

$$S_{\mu\nu}(\vec{K}) = \int_{\Omega} \chi_{\mu\vec{K}}^*(\vec{r}) \chi_{\nu\vec{K}}(\vec{r}) d\vec{r} \quad (\text{D17})$$

The  $\Omega$  in the above equations represents integration in the unit cell. The corresponding one- and two-electrons in the Hamiltonian in Eq.(1) can thus be computed from a Hartree-Fock calculation.

## ACKNOWLEDGMENTS

This work is supported by Central Research Institute, 2012 Labs, Huawei Technologies.

---

[1] J. Preskill, *Quantum* **2**, 79 (2018).  
[2] R. P. Feynman, *International Journal of Theoretical Physics* **21**, 467 (1982).  
[3] D. S. Abrams and S. Lloyd, *Physical Review Letters* **83**, 5162 (1999).  
[4] A. Aspuru-Guzik, A. D. Dutoi, P. J. Love, and M. Head-Gordon, *Science* **309**, 1704 (2005).  
[5] Y. Cao, J. Romero, J. P. Olson, M. Degroote, P. D. Johnson, M. Kieferová, I. D. Kivlichan, T. Menke, B. Peropadre, N. P. D. Sawaya, S. Sim, L. Veis, and A. Aspuru-Guzik, *Chemical Reviews* **119**, 10856 (2019).  
[6] J. Du, N. Xu, X. Peng, P. Wang, S. Wu, and D. Lu, *Phys. Rev. Lett.* **104**, 030502 (2010).  
[7] Z. Li, M.-H. Yung, H. Chen, D. Lu, J. D. Whitfield, X. Peng, A. Aspuru-Guzik, and J. Du, *Scientific Reports* **1**, 88 (2011).  
[8] B. P. Lanyon, J. D. Whitfield, G. G. Gillett, M. E. Goggin, M. P. Almeida, I. Kassal, J. D. Biamonte,

M. Mohseni, B. J. Powell, M. Barbieri, *et al.*, *Nature chemistry* **2**, 106 (2010).

[9] R. Santagati, J. Wang, A. A. Gentile, S. Paesani, N. Wiebe, J. R. McClean, S. Morley-Short, P. J. Shadbolt, D. Bonneau, J. W. Silverstone, D. P. Tew, X. Zhou, J. L. O'Brien, and M. G. Thompson, *Science Advances* **4** (2018).

[10] Y. Wang, F. Dolde, J. Biamonte, R. Babbush, V. Bergholm, S. Yang, I. Jakobi, P. Neumann, A. Aspuru-Guzik, J. D. Whitfield, and J. Wrachtrup, *ACS Nano* **9**, 7769 (2015).

[11] P. J. J. O'Malley, R. Babbush, I. D. Kivlichan, J. Romero, J. R. McClean, R. Barends, J. Kelly, P. Roushan, A. Tranter, N. Ding, B. Campbell, Y. Chen, Z. Chen, B. Chiaro, A. Dunsworth, A. G. Fowler, E. Jeffrey, E. Lucero, A. Megrant, J. Y. Mutus, M. Neeley, C. Neill, C. Quintana, D. Sank, A. Vainsencher, J. Wenner, T. C. White, P. V. Coveney, P. J. Love, H. Neven, A. Aspuru-Guzik, and J. M. Martinis, *Physical Review X* **6**, 031007 (2016).

[12] M.-H. Yung, J. Casanova, A. Mezzacapo, J. McClean, L. Lamata, A. Aspuru-Guzik, and E. Solano, *Scientific Reports* **4**, 3589 (2015).

[13] A. Peruzzo, J. McClean, P. Shadbolt, M.-H. Yung, X.-Q. Zhou, P. J. Love, A. Aspuru-Guzik, and J. L. O'Brien, *Nature Communications* **5**, 4213 (2014).

[14] A. Kandala, A. Mezzacapo, K. Temme, M. Takita, M. Brink, J. M. Chow, and J. M. Gambetta, *Nature* **549**, 242 (2017).

[15] J. I. Colless, V. V. Ramasesh, D. Dahmen, M. S. Blok, M. E. Kimchi-Schwartz, J. R. McClean, J. Carter, W. A. de Jong, and I. Siddiqi, *Physical Review X* **8**, 011021 (2018).

[16] R. Sagastizabal, X. Bonet-Monroig, M. Singh, M. A. Rol, C. C. Bultink, X. Fu, C. H. Price, V. P. Ostroukh, N. Muthusubramanian, A. Bruno, M. Beekman, N. Haider, T. E. O'Brien, and L. DiCarlo, *Phys. Rev. A* **100**, 010302 (2019).

[17] Y. Shen, X. Zhang, S. Zhang, J.-N. Zhang, M.-H. Yung, and K. Kim, *Phys. Rev. A* **95**, 020501 (2017).

[18] C. Hempel, C. Maier, J. Romero, J. McClean, T. Monz, H. Shen, P. Jurcevic, B. P. Lanyon, P. Love, R. Babbush, A. Aspuru-Guzik, R. Blatt, and C. F. Roos, *Physical Review X* **8**, 031022 (2018).

[19] Y. Nam, J.-S. Chen, N. C. Pisenti, K. Wright, C. Delaney, D. Maslov, K. R. Brown, S. Allen, J. M. Amini, J. Apisdorf, K. M. Beck, A. Blinov, V. Chaplin, M. Chmielewski, *et al.*, *npj Quantum Information* **6**, 33 (2019).

[20] I. G. Ryabinkin, R. A. Lang, S. N. Genin, and A. F. Izmaylov, *Journal of chemical theory and computation* **16**, 1055 (2020).

[21] Y. Kawashima, M. P. Coons, Y. Nam, E. Lloyd, S. Matsuura, A. J. Garza, S. Johri, L. Huntington, V. Senicourt, A. O. Maksymov, J. H. V. Nguyen, J. Kim, N. Alidoust, A. Zaribafyan, and T. Yamazaki, arXiv: 2102.07045 [quant-ph] (2021), arXiv:2102.07045 [quant-ph].

[22] J. Romero, R. Babbush, J. R. McClean, C. Hempel, P. J. Love, and A. Aspuru-Guzik, *Quantum Science and Technology* **4**, 014008 (2018).

[23] J. Lee, W. J. Huggins, M. Head-Gordon, and K. B. Whaley, *Journal of Chemical Theory and Computation* **15**, 311 (2019).

[24] H. R. Grimsley, S. E. Economou, E. Barnes, and N. J. Mayhall, *Nature Communications* **10**, 3007 (2019).

[25] W. Kutzelnigg, *The Journal of Chemical Physics* **77**, 3081 (1982).

[26] R. J. Bartlett, S. A. Kucharski, and J. Noga, *Chemical Physics Letters* **155**, 133 (1989).

[27] A. G. Taube and R. J. Bartlett, *International Journal of Quantum Chemistry* **106**, 3393 (2006).

[28] S. B. Bravyi and A. Y. Kitaev, *Annals of Physics* **298**, 210 (2002).

[29] P. Jordan and E. Wigner, *Zeitschrift für Physik* **47**, 631 (1928).

[30] A. Tranter, P. J. Love, F. Mintert, and P. V. Coveney, *Journal of Chemical Theory and Computation* **14**, 5617 (2018).

[31] J. T. Seeley, M. J. Richard, and P. J. Love, *The Journal of Chemical Physics* **137**, 224109 (2012).

[32] H. R. Grimsley, D. Claudino, S. E. Economou, E. Barnes, and N. J. Mayhall, *Journal of Chemical Theory and Computation* **16**, 1 (2020).

[33] R. Babbush, J. McClean, D. Wecker, A. Aspuru-Guzik, and N. Wiebe, *Physical Review A* **91**, 022311 (2015).

[34] Q. Sun, T. C. Berkelbach, N. S. Blunt, G. H. Booth, S. Guo, Z. Li, J. Liu, J. D. McClain, E. R. Sayfutyarova, S. Sharma, S. Wouters, and G. K.-L. Chan, *WIREs Computational Molecular Science* **8**, e1340 (2018).

[35] X.-S. Xu *et al.*, Mindquantum, <https://gitee.com/mindspore/mindquantum> (2021).

[36] P. Virtanen, R. Gommers, T. E. Oliphant, M. Haberland, T. Reddy, D. Cournapeau, E. Burovski, P. Peterson, W. Weckesser, J. Bright, S. J. van der Walt, M. Brett, J. Wilson, K. J. Millman, N. Mayorov, *et al.*, *Nature Methods* **17**, 261 (2020).

[37] D. A. Mazzotti, *Physical Review A* **69**, 012507 (2004).

[38] D. Mukherjee and W. Kutzelnigg, *Chemical Physics Letters* **397**, 174 (2004).

[39] S. Ronen, *Physical Review Letters* **91**, 123002 (2003).

[40] S. Goedecker, M. Teter, and J. Hutter, *Physical Review B* **54**, 1703 (1996).

[41] J. Liu, L. Wan, Z.-Y. Li, and J.-L. Yang, *Journal of Chemical Theory and Computation* **16**, 6904 (2020).

[42] Y. Fan, J. Liu, Z.-Y. Li, and J.-L. Yang (unpublished).

[43] D. A. Mazzotti, *Phys. Rev. A* **75**, 022505 (2007).

[44] D. Z. Manrique, I. T. Khan, K. Yamamoto, V. Wichterich, and D. M. Ramo, *Momentum-space unitary coupled cluster and translational quantum subspace expansion for periodic systems on quantum computers* (2021).

[45] H. J. Monkhorst and J. D. Pack, *Physical Review B* **13**, 5188 (1976).